Dynamics of Offset Bearings: Parametric Studies

J. F. Booker

P. Olikara

Mechanical and Aerospace Engineering,
Cornell University,
Ithaca, N.Y. 14853

Novel "offset" designs offer greatly improved durability in applications for which conventional journal bearings are only marginally satisfactory. They are particularly attractive for duty cycles which combine nonreversing loading with limited angular oscillation. Offset designs seem equally promising for steady-state operation with counter-rotation of shaft and sleeve under fixed load, or (equivalently) with load rotating at half shaft speed. Both cases are elucidated through (dimensional) numerical examples and (nondimensional) parametric studies. In both cases performance of full journal bearings is shown to be both significantly improved by small offsets and fairly insensitive to small departures from optimal values.

Introduction

Thick-film lubrication of most "self-acting" oil-lubricated bearings requires the presence of two lubrication mechanisms. Transient "squeeze" effects (which are normally cyclic in successful applications) are the direct consequences of the variation of film thickness in time: steady-state "wedge" effects arise from variation of film thickness in space in the direction of the net lubricant entrainment (convection) velocity. Both effects are local and can occur in combination.

Both temporal "squeeze" and spatial "wedge" mechanisms are entirely lacking or severely limited when conventional (full circular) bearings are applied under certain duty cycles. "Squeeze" effects can be missing entirely (in steady-state conditions) or ineffective (for lack of cyclic reversal). Convective "wedge" effects can be absent for lack of either a geometric wedge or *net* lubricant convection.

An elegant approach to such problems is the deliberate modification of bearing surface(s) such that journal rotation, however limited, results (at least locally) in one or both of the desired effects (and the consequent enhancement of thick-film lubrication). The endless design possibilities of this approach are exemplified by the elliptical bearings studied by Goenka and Booker [1983] and the offset cylindrically-segmented bearings studied by Booker, Goenka, and van Leeuwen [1982]. The present paper is concerned with further investigations of this latter bearing type.

Figure 1 shows a journal bearing in which both journal and sleeve are divided axially into cylindrical segments with "offset" centerlines. (Use of the term "eccentric" would be entirely appropriate were it not for its preemption for other uses in the tradition of journal bearing analysis.)

Though only the lower half of the sleeve is actually shown in the exploded view of Fig. 1, each cylindrical bearing segment in the present study is *complete* (in contradistinction to the partial-arc bearing segments studied by Booker et al. [1982]).

Circumferential grooves between segments (though not shown in Fig. 1) would be included in any practical design, both for lubricant distribution and ease of manufacture.

Offsets in Fig. 1 are grossly exaggerated; practical bearings with offsets comparable to clearances are visually indistinguishable from conventional circumferentially-grooved bearings.

For simplicity the prototypical offset bearing of Fig. 1 has only 2 segments; any practical arrangement would need some means of counteracting resultant film moments normal to the axis of rotation. (The complexitiy of much of the analysis which follows is included in contemplation of these more general arrangements.)

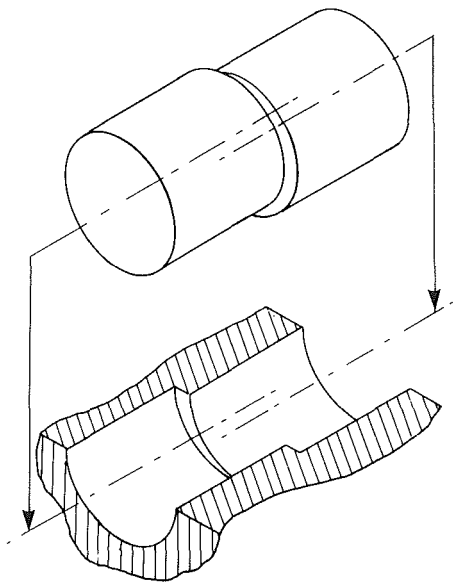

Fig. 1 Dual-center offset bearing

Contributed by the Lubrication Division of THE AMERICAN SOCIETY OF MECHANICAL ENGINEERS and presented at the ASME/ASLE Joint Lubrication Conference, Hartford, Conn., October 18–20, 1983. Manuscript received by the Lubrication Division, March 19, 1983. Paper No. 83-Lub-39.

Analysis

Following in outline[1] the analysis of Booker et al. [1982], Figure 2 shows the geometry of a typical segment from the offset bearing of Fig. 1.

Figure 2(*a*) defines four points[2]

- O : bearing reference
- P_i : bearing segment center
- O′ : journal reference
- P_i' : journal segment center

Figure 2(*b*) defines four vectors[3]

- $\mathbf{e}_0$: journal reference position
- $\mathbf{e}_i$: journal segment center position (eccentricity)
- $\mathbf{a}_i$: bearing segment center offset
- $\mathbf{b}_i$: journal segment center offset

which are related by the kinematic loop equation

$$\mathbf{e}_i - \mathbf{e}_0 = \mathbf{b}_i - \mathbf{a}_i \tag{1}$$

Figure 3 shows the superposition of two coordinate systems[4] on the journal of Fig. 2. In Fig. 3 the reference axes x',y' are fixed to and rotate with the journal through the angle ϕ relative to the reference axes x,y fixed to the sleeve. Thus offset components a_i^x, a_i^y and $b_i^{x'}$, $b_i^{y'}$ are fixed, while variable components b_i^x, b_i^y are given by the transformation

$$\begin{Bmatrix} b_i{}^x \\ b_i{}^y \end{Bmatrix} = \begin{bmatrix} \cos\phi & -\sin\phi \\ \sin\phi & \cos\phi \end{bmatrix} \begin{Bmatrix} b_i{}^{x'} \\ b_i{}^{y'} \end{Bmatrix} \tag{2}$$

In these general terms, the simple dual-center arrangement of Fig. 1 is specified by dimensions

$$\begin{aligned} L_1 &= L_2 = L \\ D_1 &= D_2 = D \\ C_1 &= C_2 = C \end{aligned} \tag{3}$$

with absolute offsets

$$\begin{aligned} a_1{}^x &= b_1{}^{x'} = 0 \\ a_1{}^y &= b_1{}^{y'} = -\delta/2 \\ a_2{}^x &= b_2{}^{x'} = 0 \\ a_2{}^y &= b_2{}^{y'} = +\delta/2 \end{aligned} \tag{4}$$

expressed in terms of relative offset δ between segment centers as shown in Fig. 4 for the simple dual-center geometry which is used throughout the present study.

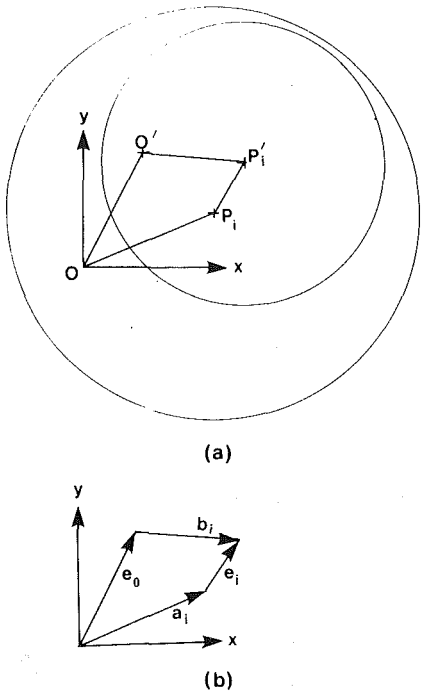

Fig. 2 Geometry of typical bearing segment

Introducing offset and rotation into the kinematic loop equation(s) (1) via relations (4) and (2), and *arbitrarily* constraining journal center motion by the symmetry condition.

$$\mathbf{e}_0 = \mathbf{0} \tag{5}$$

gives a fundamental and useful relation

$$e_i/\delta = \sin(\phi/2) \tag{6}$$

between eccentricities e_i, offset δ, and rotation ϕ in the special case of symmetrical motion.

Introducing the physical constraint(s)

$$e_i \le C \tag{7}$$

gives the limiting design relation

$$\delta \le C/\sin(\phi/2) \tag{8}$$

as plotted in Fig 5, so that for *full* rotation without interference[5]

$$e_i \le \delta \le C \tag{9}$$

(though much larger offsets are possible for *partial* rotation).

[1] The present notation is simplified somewhat.

[2] In practice, the distance between points (and thus the length of vectors) is of the order of bearing clearance, which is greatly exaggerated in Fig. 2, as the offset is in Fig. 1.

[3] See previous footnote 2.

[4] Note that in a scale drawing such as Fig. 3 (without exaggeration of offsets and eccentricities) the various centers effectively coalesce.

[5] In a similar way, the limiting design relation $\delta \le C$ is also the condition for axial assembly without interference.

Nomenclature

x, y	$[L]$	=	reference axes (sleeve)
$x'\ y'$	$[L]$	=	reference axes (journal)
t	$[T]$	=	time
T	$[-]$	=	time (dimensionless)
ϕ	$[-]$	=	journal angle
Φ	$[-]$	=	journal angle amplitude
Ω	$[T^{-1}]$	=	journal angle frequency
ω	$[T^{-1}]$	=	journal angular velocity
ω_F	$[T^{-1}]$	=	load angular velocity
β_F	$[-]$	=	load phase angle
F	$[F]$	=	total load
i	$[-]$	=	segment identifier
μ	$[FL^{-2}T]$	=	viscosity
C	$[L]$	=	radial clearance
R	$[L]$	=	radius
D	$[L]$	=	diameter
L	$[L]$	=	length
a	$[L]$	=	bearing offset
b	$[L]$	=	journal offset
δ	$[L]$	=	relative offset
e	$[L]$	=	journal eccentricity
ϵ	$[-]$	=	journal eccentricity (dimensionless)

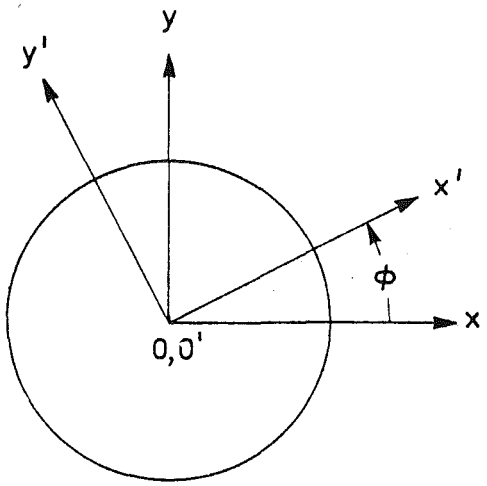

Fig. 3 Coordinate system reference axes

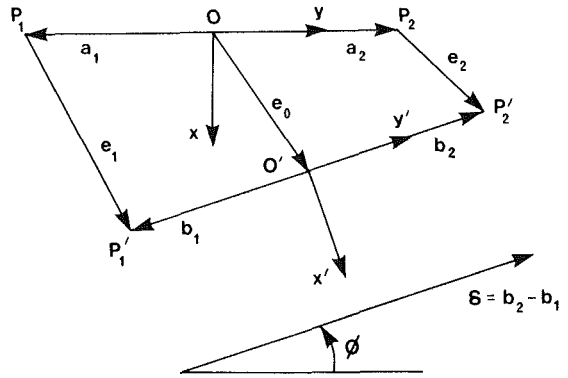

Fig. 4 Typical dual-center kinematic loop

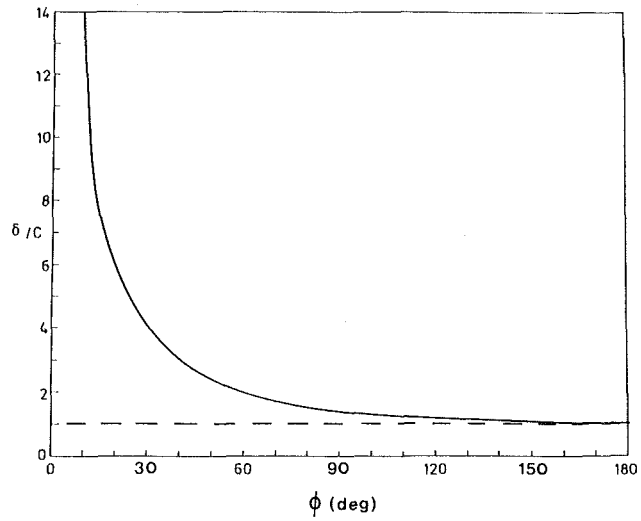

Fig. 5 Kinematic interference limit

As direct consequences of the kinematic symmetry condition (5), special relations (6), (8), and (9) provide useful insights for load-free motion in the Numerical Examples below.

Dynamic analysis of offset bearings reduces to a computational initial-value problem in which journal angular displacement and velocity and total system load are specified for all time, while journal reference point position components are specified initially and must satisfy differential equations of motion thereafter.

The system analysis, computation scheme, and computer program of Booker et al. [1982] (complemented by appropriate film property data[6] for the present complete cylindrical bearing segments) provide a ready basis for numerical solution of the problem of journal motion. (Compatible procedures for computation of friction torque and power loss are also suggested by Booker et al. [1982].)

In the numerical simulation procedure the journal reference point velocity at any time is determined such that the sum of the resulting fluid film forces computed for all (both) bearing segments exactly balances the specified applied load. Time and journal reference point position are then stepped ahead[7] and the process repeated.

Previous Applications

Booker, Goenka, and van Leeuwen [1982] provide both a very general analysis and very specific numerical studies of applications of "offset" designs to piston (and/or cross-head) pin bearings for two different 2-stroke Diesel engines, together with a literature survey of commercial implementations.

Concurrently and independently, Wakuri, Ono, and Soejima [1982] report apparently similar studies. Unfortunately, their numerical study of a large production engine (also studied by Booker et al. [1982]) neglects the presence of *sleeve* segment offset—an important feature of practical designs.

Thus all previously published numerical studies[8] of offset bearings involve dimensional studies of specific engine applications.

The dimensional and nondimensional parametric studies of simple prototypical problems carried out by Olikara [1981] allow a clearer understanding of basic mechanisms and indicate some of the further potential of the offset bearing. These studies, based on the analysis outlined above, are excerpted in the two Numerical Examples which follow.

Numerical Example I: Journal Oscillating, Load Fixed

The basic "offset" design approach already taken to production piston-pin/wrist-pin bearings in 2-stroke engines should apply equally well to many other applications (such as rocker arms) with duty cycles which also combine nonreversing loading with limited angular oscillation.

The simplest prototypical example of this situation combines steady loading with sinusoidal angular oscillation in the duty cycle

$$\begin{aligned} F^x &= F \\ F^y &= 0 \\ \phi &= \Phi \sin(\Omega t) \end{aligned} \tag{10}$$

Theoretical results of both Gupta and Phelan [1964] and Goenka and Booker [1983] show extremely low load capacities for conventional bearings operating under such duty cycles; published experimental results of others reviewed by Gupta and Phelan [1964] allow similar conclusions. Inadequacy of "squeeze" and "wedge" effects makes satisfactory periodic operation unlikely for conventional bearings. Olikara [1981], however, predicts considerable capacities for offset designs under these circumstances.

[6] Appropriate "π short bearing" film force components used throughout the present study are given (for example) by Badgley and Booker [1969] and by Childs, Moes, and van Leeuwen [1977]. The latter derivation (published with extensive complementary discussion by Booker) follows the "impedance" format, in which film force data are given by Moes and Bosma [1981] for models other than the π short bearing used here.

[7] Throughout the present study the stepping procedure is linear (Euler) extrapolation with a step size corresponding to 1/2 degree in dimensionless time.

[8] Excluded are previous studies of bearings with only sleeve offsets.

Figures 6-8 show the predicted periodic[9] response of a sample (offset) bearing design to a sample duty cycle specified by the parameters of Table 1(*a*).

Figure 6 shows the resulting periodic orbits the two journal centers follow within their clearance spaces (while maintaining a fixed relationship to one another). Circles mark 1/8-cycle intervals, with arrowheads indicating the cyclic progression. (The superimposed vector diagrams show the instantaneous configuration at the 1/8-cycle point.) The two orbits are seen to be mirror images, as might be expected from the symmetry of the problem. Their shape is very different from the severely flattened "figure eights" of Gupta and Phelan [1964] for a similar case without offset.

Figures 7(*a*) and (*b*) display the corresponding displacement components against time throughout the cycle. (The 1/8-cycle point is marked by an arrow.) With their disparate scales, the two components illustrate the essentially one-dimensional character of the motion, showing periods of squeezing alternating with periods of recovery.

Figures 8(*a*) and (*b*) show the corresponding film load components throughout the cycle. The disparate scales used for the components emphasize again the essentially one-dimensional character of the problem. The *net* load is, of course, constant, being unrelieved throughout the cycle. However, the *individual* loads borne by the two segments *are* relieved periodically. Note the close correlation of these loads with the corresponding rates-of-change of segment center displacements shown in Figs. 7(*a*) and (*b*).

[9] Periodicity is achieved by running the simulation over multiple duty cycles and/or modifying (arbitrary) initial conditions.

Table 1 Sample duty cycle/bearing design (Numerical Example I)

(*a*) Dimensional parameters

$F = 1000.$ N
$\Omega = 100.$ rad/s
$\Phi = \pi/4$ rad

$\mu = 10. \times 10^{-3}$ Ns/m^2
$L = 20. \times 10^{-3}$ m
$D = 20. \times 10^{-3}$ m
$C = 20. \times 10^{-6}$ m
$\delta = 18. \times 10^{-6}$ m

(*b*) Nondimensional parameters

$$\frac{F(C/R)^2}{LD\mu\Omega} = 10.$$

$L/D = 1.$
$\delta/C = 0.9$
$\Phi = \pi/4$

Nondimensional Parameterization. Expressing the 8 dimensional parameters of Table 1(*a*) in terms of the 4 nondimensional parameters[10] of Table 1(*b*) provides a sufficient basis for calculation of nondimensional displacement response

$$\epsilon = e/C$$

in terms of nondimensional time

$$T = \Omega t$$

The results of the sample simulation defined in Table 1(*b*) and displayed in Figs. 6 and 7 are plotted as a single point (solid circle) in Fig. 9, which shows the dependence of cyclically-extreme values of (dimensionless) journal displacement on (dimensionless) journal offset and angular amplitude; other dimensionless parameters are as given in Table 1(*b*). This figure shows *both* the benefits of even small offsets *and* the detriments of approach (at high offsets and/or angular excursions) to the kinematic limit of physical interference suggested by equation (8) and Fig. 5.

Results of the sample simulation are again plotted as a single point in Fig. 10, which shows the dependence of extreme values of journal displacement on offset and load; other dimensionless parameters are again as given in Table 1(*b*). For this figure the zero-load data are given by the relation (6) developed above for symmetrical motion.

Complete data for the zero-offset case are missing from Fig. 10, owing to the unusually high computational expense involved in obtaining periodic responses at high eccentricities (though Gupta and Phelan [1964] do provide a half-dozen such data points). As it is, Figs. 9-10 show cyclic extremes representing scores of individual simulations.

[10] If (as here) the analysis is based on the short bearing approximation, the nondimensional load and aspect ratio parameters can be further combined into a single nondimensional parameter.

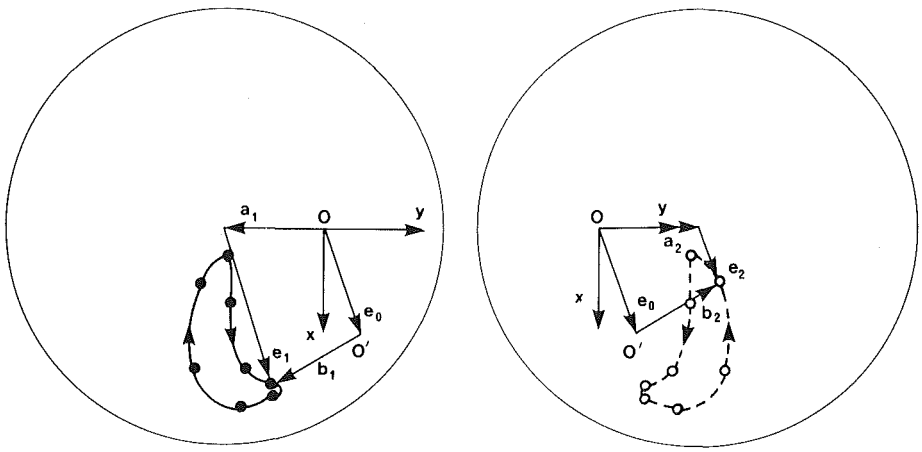

Fig. 6 Journal center paths (Numerical Example I)
(*a*) Segment 1
(*b*) Segment 2

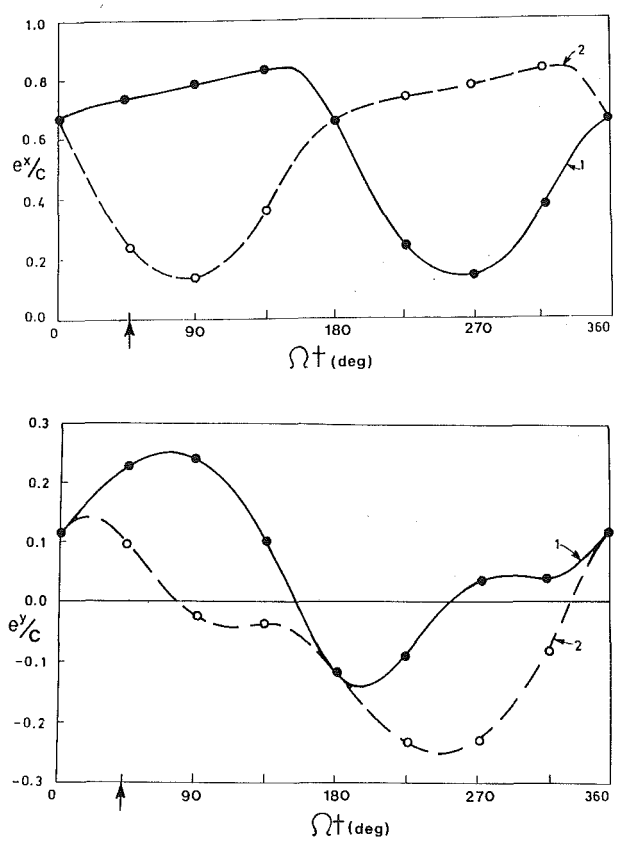

Fig. 7 Journal center eccentricity components versus time (Numerical Example I)

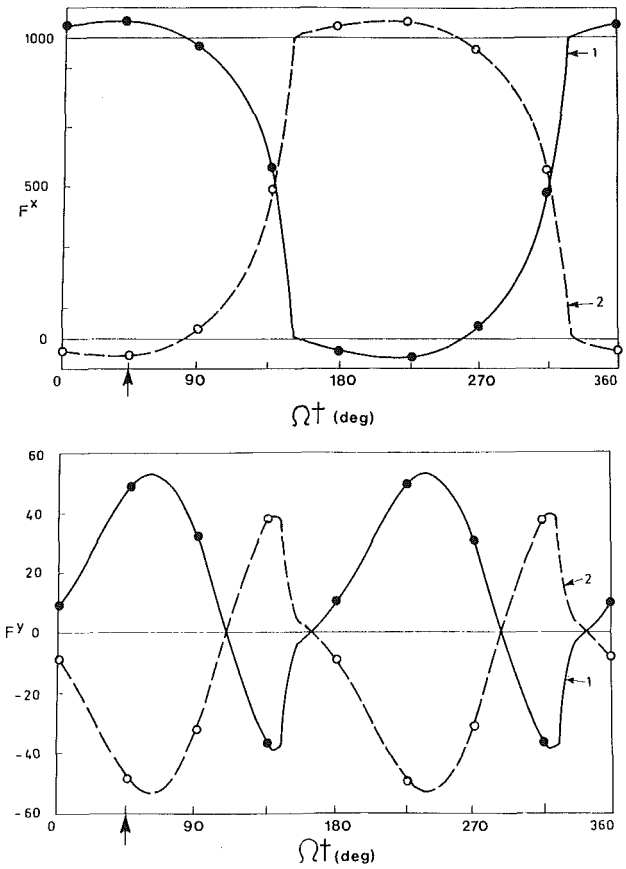

Fig. 8 Film load components versus time (Numerical Example I)

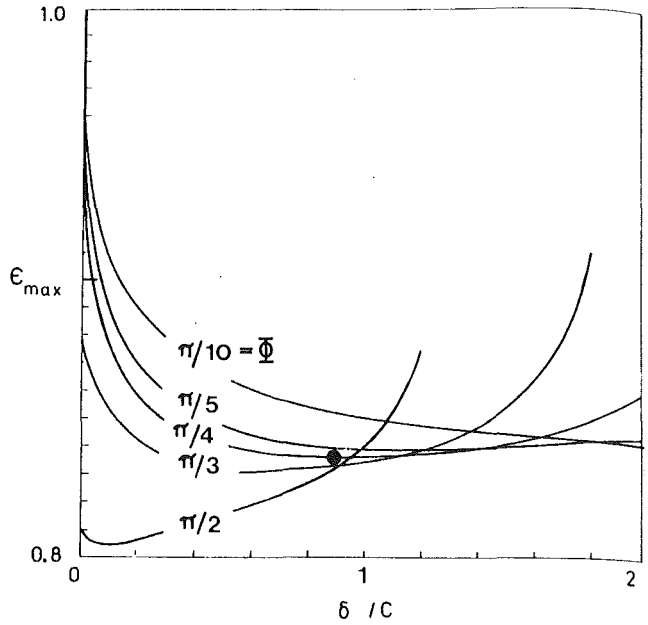

Fig. 9 Maximum journal center eccentricity versus offset and angle amplitude: unlisted parameters as in Table 1(*b*) (Numerical Example I)

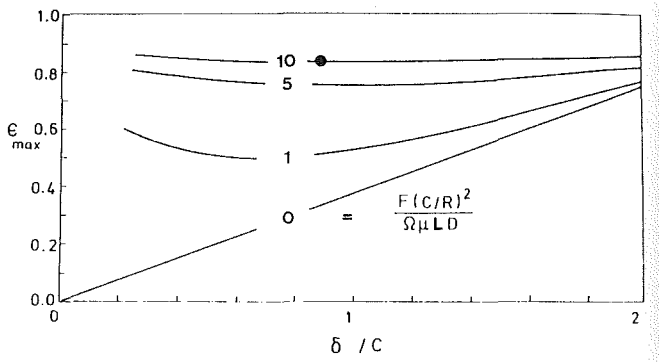

Fig. 10 Maximum journal center eccentricity versus offset and load: unlisted parameters as in Table 1(*b*) (Numerical Example I)

Numerical Example II: Journal Rotating, Load Rotating

Conventional bearings are also only marginally satisfactory in steady-state operation with loads rotating at or near 1/2 shaft speed.

The simplest prototypical example of this situation combines steady rotation of journal and load in the duty cycle

$$\begin{aligned} \phi &= \omega t \\ F^x &= F\cos(\omega_F t + \beta_F) \\ F^y &= F\sin(\omega_F t + \beta_F) \end{aligned} \tag{11}$$

Pinkus [1962] has shown, both theoretically and experimentally, that plain (full circular) journal bearings are unsatisfactory for the (equivalent) case of steady counter-rotation of shaft and sleeve under fixed load. Absence of "squeeze" and "wedge" effects (and/or *net* convective flow) makes satisfactory steady-state operation well-neigh impossible for conventional bearings. Olikara [1981], however, predicts considerable capacities for "offset" designs operating under such duty cycles as that given above.

[11] See previous footnote 9.

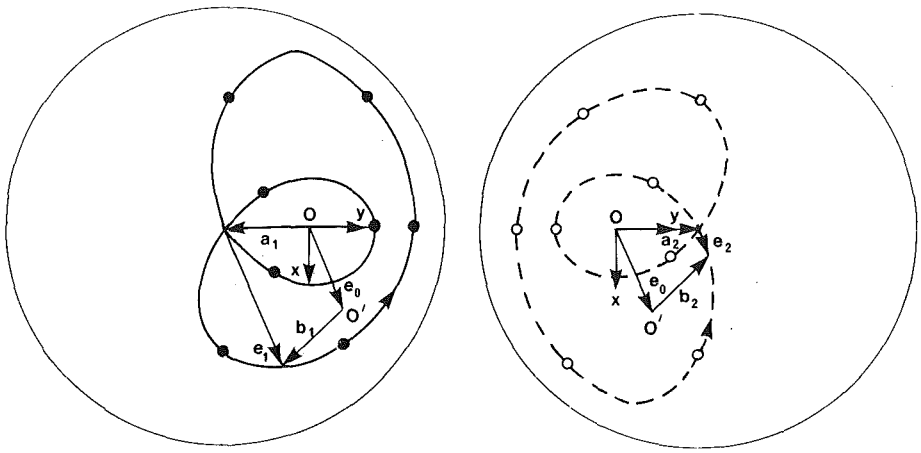

Fig. 11 Journal center paths
(Numerical Example II)
(a) Segment 1
(b) Segment 2

Table 2 Sample duty cycle/bearing design (Numerical Example II)

(a) Dimensional parameters

F	=	1000.	N
ω_F	=	100.	rad/s
β_F	=	$\pi/2$	rad
ω	=	200.	rad/s
μ	=	$10.\times10^{-3}$	Ns/m^2
L	=	$10.\times10^{-3}$	m
D	=	$20.\times10^{-3}$	m
C	=	$20.\times10^{-6}$	m
δ	=	$15.\times10^{-6}$	m

(b) Nondimensional parameters

$$\frac{2F(C/R)^2}{LD\mu\omega} = 10.$$

$$L/D = 1.$$
$$\delta/C = 0.75$$
$$\omega_F/\omega = 0.5$$
$$\beta_F = \pi/2$$

Figures 11–12 show the predicted periodic[11] response of a sample (offset) bearing design to a sample duty cycle specified by the parameters of Table 2(*a*). (Note that, except for offsets, the sample bearing designs of Tables 1 and 2 are identical.)

Figure 11 shows the resulting periodic orbits the two journal centers follow within their clearance spaces (while maintaining a fixed relationship to one another). Circles mark 1/8-cycle intervals, with arrowheads indicating the cyclic progression.[12] (The superimposed vector diagrams shows the instantaneous configuration at the 1/16-cycle point.) The two orbits are seen to be identical, though shifted, as expected from the symmetry of the problem.

Figure 12 displays the corresponding displacements (eccentricities) against time or shaft rotation through the cycle. (The 1/16-cycle point is marked by an arrow.)

Nondimensional Parameterization. Expressing the 9 dimensional parameters of Table 2(*a*) in terms of the 5 nondimensional parameters[13] of Table 2(*b*) provides a sufficient basis for calculation of nondimensional displacement response

$$\epsilon = e/C$$

in terms of nondimensional time

$$T = |\omega| t$$

[12] 1/8 cycle of 1/2-speed loading corresponds to 1/4 shaft rotation.
[13] See previous footnote 10.

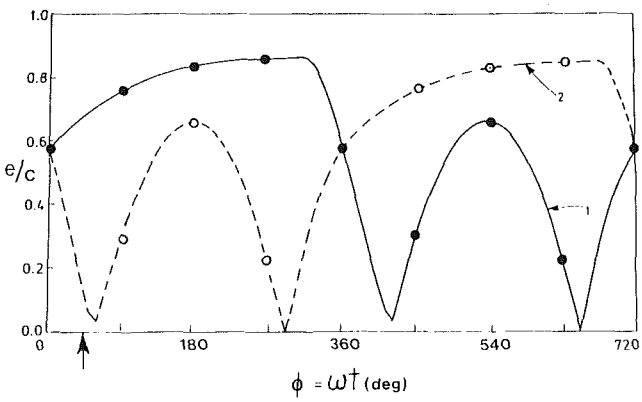

Fig. 12 Journal center eccentricities versus time
(Numerical Example II)

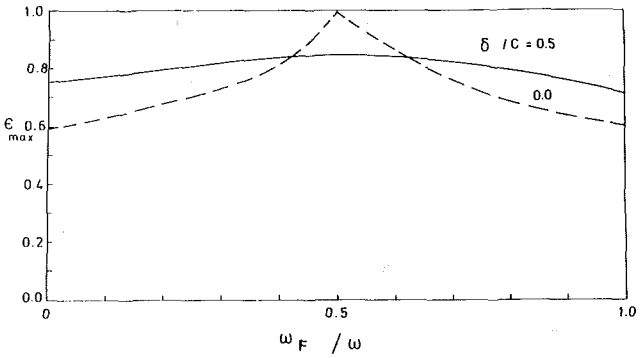

Fig. 13 Maximum journal center eccentricity versus angular velocity and offset: unlisted parameters as in Table 2(*b*)
(Numerical Example II)

Figure 13 shows the dependence of cyclically-extreme values of journal displacement on offset and load angular velocity; at the critical "half-speed" condition the superiority of the offset bearing is evident. Other dimensionless parameters are as given in Table 2(*b*).

Load phase angle is defined by equation (11) as the initial angle of the load direction relative to the shaft offset direction. At least for half-speed loading it appears that load phase angle is not a very important parameter; predicted displacement is least for phase angle 0 and greatest for phase angle $\pi/2$ (as in the cases shown here).

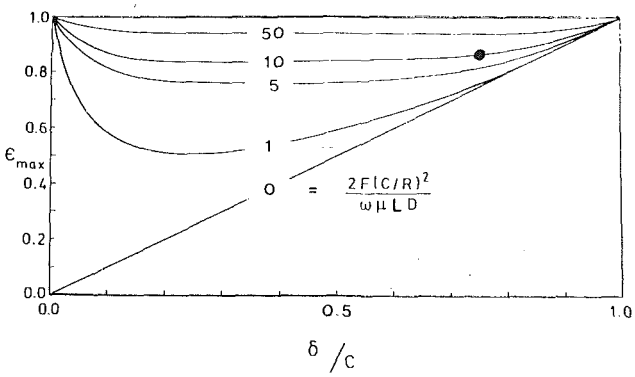

Fig. 14 Maximum journal center eccentricity versus offset and load: unlisted parameters as in Table 2(*b*) (Numerical Example II)

The results of the sample simulation defined in Table 2(*b*) and displayed in Figs. 11 and 12 are plotted as a single point in Fig. 14, which shows the dependence of maximum displacement on offsets and loads at the half-speed load condition. The zero-load curve is again given by the relation (6) developed above for symmetrical motion. The results shown suggest that even small values of offset can be beneficial, and that small deviations from optimal values are unimportant.

Summary and Conclusions

Novel "offset" designs appear to offer greatly improved durability in applications for which conventional journal bearings are only marginally satisfactory.

They are particularly attractive for duty cycles which combine nonreversing loading with limited angular oscillation.

Offset designs seem equally promising for steady-state operation with counter-rotation of shaft and sleeve under fixed load, or (equivalently) with load rotating at half shaft speed.

Prototypical Numerical Examples of both application types include both specific dimensional cases and quite general nondimensional parametric studies representing about 100 individual simulations.

In both Numerical Examples performance of full journal bearings is shown to be both significantly improved by small offsets and fairly insensitive to small departures from optimal values.

Recommendations for Future Work

Specific practical applications of both types set out here in prototypical Examples deserve further study (both theoretical and experimental).

Numerical Example I suggests application to reciprocating machinery, with the examination of rocker arm bearings as well as further study of wrist-pin bearings.

Numerical Example II suggests application to rotating machinery, noting particularly the favorable stability implications of the observed insensitivity to half-speed load rotation.

More complex arrangements of centers (e.g. triple-center bearings) and possibilities for reduced power loss (under enhanced thick-film conditions) should be explored for both types of machinery.

Acknowledgments

The authors are deeply indebted to two institutions and their personnel:

- - - Cornell University, USA,
where the work was carried out
- - - Durham University, UK,
where this publication was prepared.

References

1962 Pinkus, O., "Counterrotating Journal Bearings," ASME *Journal of Basic Engineering*, Vol. 84, No. 1, March 1962, pp. 110–118.

1964 Gupta, B. K., and Phelan, R. M., "The Load Capacity of Short Journal Bearings with Oscillating Effective Speed," ASME *Journal of Basic Engineering*, Vol. 86, No. 2, June 1964, pp. 348–354.

1969 Badgley, R. H., and Booker, J. F., "Turborotor Instability—Effect of Initial Transients on Plane Motion," ASME *Journal of Lubrication Technology*, Vol. 91, No. 4, Oct. 1969, pp. 625–633.

1977 Childs, D., Moes, H., and van Leeuwen, H., "Journal Bearing Impedance Descriptions for Rotordynamic Applications," ASME JOURNAL OF LUBRICATION TECHNOLOGY, Vol. 99, No. 2, Apr. 1977, pp. 198–213.

1981 Moes, H., and Bosma, R., "Mobility and Impedance Definitions for Plain Journal Bearings," ASME JOURNAL OF LUBRICATION TECHNOLOGY, Vol. 103, No. 3, July 1981, pp. 468–470.

1981 Olikara, P., "Dynamics of Offset Bearings," M.S. thesis, Cornell University, Ithaca, N.Y., Jan. 1981.

1982 Booker, J. F., Goenka, P. K., and van Leeuwen, H. J., "Dynamic Analysis of Rocking Journal Bearings with Multiple Offset Segments," ASME JOURNAL OF LUBRICATION TECHNOLOGY, Vol. 104, No. 4, Oct. 1982, pp. 478–490. Addendum, Vol. 105, No. 2, April 1983, p. 220.

1982 Wakuri, Y., Ono, S., and Soejima, M., "On the Lubrication of Crosshead-pin Bearing with Eccentric Journal," *Bulletin of the JSME*, Vol. 25, No. 206, Aug. 1982, pp. 1312–1320.

1983 Goenka, P. K., and Booker, J. F., "Effect of Surface Ellipticity on Dynamically Loaded Cylindrical Bearings," ASME JOURNAL OF LUBRICATION TECHNOLOGY, Vol. 105, No. 1, Jan. 1983, pp. 1–12.